*Desalination and Water Treatment*
www.deswater.com

doi: 10.5004/dwt.2019.24004

154 (2019) 82–91
June

# $NH_2$-grafting on micro/nano architecture designed PS/TPU@$SiO_2$ electrospun microfiber membrane for adsorption of Cr(VI)

Bin Wang[a,b], Zhiming Sun[c,*], Tong Liu[a], Qizhi Wang[a,b], Congju Li[d], Xiuyan Li[a,*]

[a]*School of Materials Science & Engineering, Beijing Institute of Fashion Technology, Beijing 100029, China, Tel. +86 10 64288178; email: clylxyan@bift.edu.cn (X. Li)*
[b]*Beijing Key Laboratory of Clothing Materials R & D and Assessment, Beijing Engineering Research Center of Textile Nanofiber, Beijing Institute of Fashion Technology, Beijing 100029, China*
[c]*School of Chemical and Environmental Engineering, China University of Mining and Technology (Beijing), Beijing 100083, China, Tel. +86 10 62339920; email: zhimingsun@cumtb.edu.cn*
[d]*Beijing Institute of Nanoenergy and Nanosystems, Chinese Academy of Sciences, Beijing 100083, China*

Received 20 September 2018; Accepted 20 February 2019

## ABSTRACT

Removal of hexavalent chromium [Cr(VI)] from surface water is a key problem in environmental remediation due to its carcinogenicity and mutagenicity to living organisms. In this work, we developed an effective adsorbent for Cr(VI) removal by incorporating $SiO_2$ nanospheres into electrospun microfiber membrane (polystyrene/thermoplastic polyurethane) and then modifying with amine-terminated organosilicon (3-aminopropyltriethoxysilane, APTES). The obtained aminated composite microfiber membranes exhibited unique multi-dimensional micro/nano architecture and possessed high adsorption capacity and removal efficiency for Cr(VI). Results shown that the adsorption capacity can reach 57.73 mg $g^{-1}$, moreover, removal efficiency could be maintained over 60% after three cycles of regeneration. Interestingly, the $SiO_2$ nanospheres were distributed along the polymeric microfiber uniformly, which created more surface hydroxyl groups interacted with amine groups ($-NH_2$), leading to more active $-NH_2$ terminal groups graft on the membrane surface and higher Cr(VI) adsorption capacity. Furthermore, the incorporation of $SiO_2$ nanospheres did not deprive the flexibility of electrospun microfiber membranes. The results provided new insights for the removal of heavy metal ions by multi-scaled micro/nano structured fibrous membranes from wastewater with high adsorption capacity and well recyclability.

*Keywords:* Electrospinning; Membrane; Adsorption; Hexavalent chromium

## 1. Introduction

For decades, large quantities of wastewater containing toxic heavy metal ions have been discharged into the environment irresponsibly. Surface water and groundwater are continuously polluted and clean drinking water is diminishing. Among these toxic heavy metal ions, hexavalent chromium [Cr(VI)] is generated by many processing technologies, such as the electroplating, leather tanning, steel fabrication, textile industries and chromate preparation. And also, Cr(VI) is posing great threat on living organisms, since it is toxic, not biodegradable and can accumulate in living tissues [1]. Long-term interaction with Cr(VI) can cause health problems, such as vomiting, severe diarrhea, liver damage, pulmonary congestions, and any type of cancer [2]. The treatment of Cr(VI) is of special concern due to its deleterious impact on ecosystems and human beings. Conventional methods used to remove Cr(VI) from surface water and groundwater usually include adsorption, chemical precipitation, reverse osmosis, ion exchange, membrane

---

* Corresponding authors.

filtration and photocatalytic reduction [3,4]. Among them, adsorption is found to be a promising technique for Cr(VI) removal from wastewaters due to its easy operation, low cost and high efficiency, particularly the demonstrated effectiveness various adsorbents for Cr(VI) removal from very dilute solution [5].

In recent years, nanostructured adsorbents stand out for their high efficiency owing to sufficient specific surface area from extensive porous structure for physical absorption and unique surface chemistry from surface modification for chemisorption. Many types of nano adsorbent have been explored and confirmed to exhibit excellent ability in Cr(VI) removal, for example, chitosan modified $Fe^0$ nanowires [6], titania beads [5], iron oxide nanostructures [7] and polyacrylonitrile/ferrous chloride [8]. However, these nanostructured adsorbents, especially nanoparticles, exhibited a relatively high possibility to aggregate in aqueous solution, which deprived them of excellent absorption properties; and did not have the ability to separate them from wastewater and recycle, which restrict their practical application. More recently, magnetic adsorbents have been demonstrated, including chitosan-bounded $Fe_3O_4$ nanoparticles [9], $Fe@Fe_2O_3$ core-shell nanowires [10], magnetic hydroxyapatite nanoparticles [11], amino-functionalized $Fe_3O_4@SiO_2$ core-shell magnetic nanomaterial [12], and MnO-$Fe_2O_3$ composite powders [13]. However, these nanostructured adsorbents either are synthesized by processes involving difficulties or needed to be collected by external magnetic field. Hence, it is of great importance to synthesize efficient adsorbents with facile technology and easy solid–liquid separation property.

Along this line, designing multi-dimensional micro/nano architecture would be the most promising strategy in highly-efficient adsorbents since it can meet the need to practical applications. The multi-dimensional micro/nanostructured adsorbents (e.g., 3D structured nanofibrous membranes) have previously been achieved because they can be separated from the liquids more easily than powders, because of their macroscopical boundary dimension [14–18]. For example, our group prepared hierarchically nanofibrous membranes containing thermal plastic elastomer ester or polyamide (PA6) nanofibers core and iron oxides shell via an electrospinning technology combined hydrothermal techniques, and proved their high adsorption ability for the removal of Cr(VI) [2,19]. And also, their easy solid–liquid separation property and recyclability were exhibited by repeating the Cr(VI) removal experiment for several times.

Unfortunately, merely adsorption depended on the active nano-oxides shell is insufficient and unstable for removal of heavy metal ions since this dopant shell is loaded by single-layer on electrospun nanofibers at most. As we known that electrospun nanofibrous membrane stands out for preparing functional materials with tunable architecture and surface chemistry, such as polyetherimide-silica fibrous membrane with effective filtration of fine particles [20], flexible $ZrO_2$ nanoparticle embedded nanofibrous membrane with efficient removal property for phosphate [21], amino-functionalized cellulose acetate/silica composite nanofibrous membranes for Cr(VI) removal [22], etc. Therefore, methods to increase the adsorption of heavy metal ions on electrospun fibrous membrane include enlarging the surface area and grafting functional groups on the surface.

In this work, we aimed to develop a novel $NH_2$-grafting flexible polystyrene/thermoplastic polyurethane@silica composite microfiber membrane (PS/TPU@$SiO_2$) with high adsorption capacity as an efficient adsorbent for practical application in wastewater treatment. The composite membrane was prepared by combining sol-gel, hydrothermal and electrospinning methods. The adsorption properties were demonstrated based on the removal of Cr(VI) from aqueous solution. The $SiO_2$ nanospheres distributed uniformly along the microfibers, which created more surface hydroxyl groups interacted with 3-aminopropyltriethoxysilane (APTES), leading to more active $-NH_2$ terminal groups on the composite membrane surface and higher Cr(VI) removal capacity. The as-prepared composite membrane exhibited high flexibility and recyclability. Herein we propose a facile strategy for modifying electrospun membrane with inorganic dopant decoration and surface chemistry grafting in order to enhance its adsorption capacity.

## 2. Materials and methods

### 2.1. Materials and chemicals

Polystyrene (PS, $M_r$ = 192,000 kg $kmol^{-1}$) was purchased from the Sigma-Aldrich (Shanghai, China) and thermoplastic polyurethane (TPU, Desmopan DP 2590A) was purchased from Bayer MaterialScience (Shanghai, China). Tetraethoxysilane (TEOS), N,N-dimethylacetamide (DMAc), APTES, $K_2Cr_2O_7$ (analytical reagent grade), ninhydrin, sodium hydroxide, hydrochloric acid and ammonium hydroxide were provided by Sinopharm Chemical Reagent Company (Shanghai, China). All the above materials were used without further purification. Deionized water was used throughout this work.

### 2.2. Preparation of $SiO_2$ nanospheres

The uniform silica nanospheres were synthesized by a typical sol-gel process, reported by Wang et al. [23]. First, 1.5 mL of TEOS was added into a water/ethanol (v/v = 50/1) composite solution drop by drop. Under continuous stirring at 40°C, 6.0 mL of ammonium hydroxide was added as catalyst for hydrolysis and the resulting hydrogel were obtained after 12 h. Finally, the as-prepared silica hydrogel was dried at room temperature, and the silica nanospheres with controllable particle size and narrow size distribution were achieved (as shown in Fig. 2).

### 2.3. Preparation of electrospun PS/TPU@$SiO_2$ composite microfiber membranes

In a typical electrospinning process, a precursor solution should be prepared firstly [24]. 1.652 g PS and 0.708 g TPU were dissolved in 10 mL DMAc and stirred continuously for 12 h to make transparent PS/TPU solution. The various weights of $SiO_2$ nanospheres (0.5, 1.0, 1.5, 2.0 and 2.5 g) were added into five undefiled glass bottles with PS/TPU solution, respectively. And then the above solution was stirred subsequently for 12 h to prepare electrospinning solution. In addition, to ensure the homogeneous dispersion, ultrasonic treatment was employed for 30 min. The as-prepared solution was fed into a 10 mL syringe (Harvard Apparatus, PHD ULTRATM, Instech Solomon, USA) equipped in a home-made electrospinning machine. During fabrication of PS/TPU@$SiO_2$ composite microfiber membrane, the applied voltage was 20.0 kV, the feed rate was set at 0.5 mL $h^{-1}$ and the distance between the syringe and collector was adjusted to 15.0 cm. The electrospinning process was conducted at 40°C and 30% relative humidity. After completing the electrospinning, the membranes were dried in a vacuum oven at 70°C for 24 h to remove the residual solvent. The resultant electrospun membranes containing various $SiO_2$ nanospheres contents of 0.5, 1.0, 1.5, 2.0 and 2.5 g were denoted as PTS-0.5, PTS-1.0, PTS-1.5, PTS-2.0 and PTS-2.5. The pristine PS/TPU microfiber membrane (PTS-0) was also prepared under the same condition without adding $SiO_2$ particles in PS/TPU solution.

### 2.4. Surface modification of electrospun PS/TPU@$SiO_2$ composite microfiber membranes

The preparation of $NH_2$-grafting PS/TPU@$SiO_2$ composite microfiber membranes consist of two steps. First, silane coupling agent containing 0.5%, 1.0%, 1.5%, 2.0% and 2.5% (v/v) of APTES were prepared by dissolving in 100 mL ethanol. Second, immersing the as-spun PS/TPU@$SiO_2$ composite microfiber membranes in silane coupling agent to make $-NH_2$ groups graft on the surface of silica (Fig. 1). The reaction parameters were varied between 40°C, 50°C and 60°C when the reaction time was 12, 24, 36, 48 and 60 h, respectively. After modifying reaction, the membranes were rinsed by deionized water for three times and then dried in a vacuum oven at 70°C for 24 h to remove the residual agent.

### 2.5. Hexavalent chloride adsorption experiments

In the batch adsorption experiments, simulated Cr(VI) solution was prepared by dissolving $K_2Cr_2O_7$ in deionized water. The pH values were adjusted by 0.5 mol $L^{-1}$ HCl solution and/or 0.5 mol $L^{-1}$ NaOH solution to 2 during all the following Cr(VI) removal experiments, in order to obtain the optimal adsorption capacity (Fig. S1). For studying the removal efficiency of as-prepared electrospun microfiber membranes with different surface modification conditions, 0.01 g of membrane was immersed into 0.1 L of $K_2Cr_2O_7$ solution (40.0 mg $L^{-1}$) at room temperature, followed by sampling the solution at defined time intervals for analyzing Cr(VI) concentration change. Equilibrium time was determined from the above adsorption kinetic experiments. When the adsorption equilibrium was achieved, the Cr(VI) concentration was measured by inductively coupled plasma-atomic emission spectroscopy (ICP-AES, Prodigy, USA). The adsorption capacity of the relevant membrane for Cr(VI) was calculated as follows:

$$q_e = \frac{C_o - C_e}{m} \times V \quad (1)$$

where $q_e$ is the equilibrium adsorption quantity (mg $g^{-1}$), $C_0$ and $C_e$ represent the initial and equilibrium Cr(VI) concentration (mg $L^{-1}$), respectively. $m$ is the weight of membrane (g) and $V$ is the volume of $K_2Cr_2O_7$ solution (L).

For the regeneration, the Cr(VI) saturated membrane was immersed into 0.1 L of 0.1 mol $L^{-1}$ NaOH solution for 6 h, and then was rinsed with deionized water three times. The regenerated membrane was then reused for three consecutive cycles of Cr(VI) adsorption.

### 2.6. Measurements and characterization

The surface morphology of $SiO_2$ nanospheres and the membranes was observed through a scanning electron microscope (SEM, JEM-7500F, JEOL Ltd., Japan). The nanosphere diameter and fiber diameter were gauged employing a custom code image analysis program (Smile View). A Nicolet 6700 FT-IR spectrometer in attenuated total reflectance model with a resolution of 4 $cm^{-1}$ and in the range of 4,000–400 $cm^{-1}$ was employed to testify the presence of the grafted $-NH_2$ groups on the modified composite membranes. The as-prepared $SiO_2$ nanospheres and the membranes with and without $SiO_2$ nanospheres were detected by X-ray diffractometer (D/MAX-IIIA, Rigaku, Japan) using Cu $K\alpha$ radiation source ($\lambda$ = 1.54056 Å) at a scan rate of 5° $min^{-1}$ and XRD pattern-processing software (MDI/Jade 5.0, Materials Data, USA) was used to determine the phase composition and crystallinity. The acceleration voltage and beam current were 40 kV and 200 mA, respectively. The concentration change of Cr(VI) in aqueous solution was investigated by ICP-AES (Prodigy, USA).

## 3. Results and discussion

### 3.1. Sample characterization

The $SiO_2$ nanospheres with controllable diameter and narrow diameter distribution were synthesized by a typical

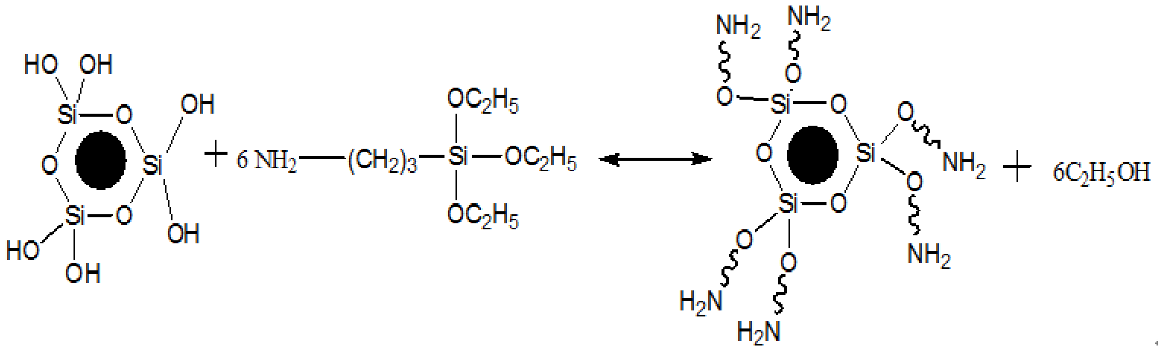

Fig. 1. Reaction schemes between APTES and hydroxyl groups of $SiO_2$ nanosphere surface.

sol-gel process in this work. The SEM image and diameter histogram of synthesized $SiO_2$ nanospheres are shown in Fig. 2. SEM characterization confirms the spherical shape of the $SiO_2$ (Fig. 2a) and reveals that these spheres possess clear boundary. The diameter of $SiO_2$ nanosphere was measured and shown in Fig. 2b, and the particle diameter distribution obeys Gaussian law with an average diameter of 150.5 nm. The crystalline structure of synthesized $SiO_2$ nanospheres is shown in Fig. 4 (line b), in where the peak occurs at 2θ = 20°–30° corresponding to the characteristic peak of silica (JCPDS No. 29-0085).

Different amounts of $SiO_2$ nanospheres were added into the PS/TPU microfibers to determine the highest doping content that could be incorporated. The morphology and $SiO_2$ nanospheres distribution in PS/TPU@$SiO_2$ microfiber membranes are displayed in Fig. 3. It illustrates that the membranes have randomly interconnected structure with no beads formed and uniform distribution of the fiber diameter and $SiO_2$ nanospheres even when the doping content reached 2.5 g (which corresponds to the total amount of polymer). This is because the diameters of the pristine fibers are in micron range and the diameters of the $SiO_2$ nanospheres are about 150 nm. Moreover, with the increasing doping content the diameter of composite fiber is slightly increased, attributing to the reasonable distribution of $SiO_2$ nanospheres as well. Under the supporting effect of electrospun microfibers, $SiO_2$ nanospheres embed uniformly onto the surface of microfiber rather than immersing into microfiber matrix or aggregate with each other, which can offer more active surface hydroxyl to react with APTES. As presented in Fig. 3g, after being doped with $SiO_2$ nanospheres the morphology of the resultant membranes was significantly endowed with multi-dimensional micro/nano rough structures on the microfibers surfaces, which indicates that the amino groups on $SiO_2$ nanospheres surface would interact with Cr(VI) intimately and effectively.

The structural and chemical changes of prepared $NH_2$-grafting PS/TPU@$SiO_2$ composite microfiber membranes induced by the incorporation of $SiO_2$ nanospheres were characterized using X-ray diffraction (XRD) analysis and FT-IR analysis, respectively. According to the XRD measurements shown in Fig. 4, a broad peak for amorphous polymer occurs at 2θ = 10°–30° corresponding to broad diffraction peak of pristine PS/TPU microfiber (line a). By the addition of 2.0 g silica, the XRD peak of PTS-2 (line c) was broadened to some extent with heightened intensity, although the position of the corresponding hybrid peak did not shift obviously upon incorporation of $SiO_2$, which demonstrates an increase in the amorphous character of the composite microfibers and implies the doping of prepared $SiO_2$ nanospheres.

FT-IR spectral analysis was employed to investigate the elemental composition of the membranes, which could testify the presence of amino-functionalized $SiO_2$ nanospheres. The FT-IR spectra for pristine PS/TPU microfiber membranes, synthesized $SiO_2$ nanospheres, PTS-2 composite microfiber membranes and amino-functionalized PTS-2 composite microfiber membranes are shown in Fig. 5. The characteristic peaks around 1,650–1,450; 3,100–2,900 and 770–730 $cm^{-1}$ corresponded to the vibration of benzene skeleton and stretching vibration of C–H bond of benzene, which are assigned to PS component (line a). The characteristic peak of Si–OH is presented at 3,450 $cm^{-1}$ and the characteristic peaks around 1,100 and 950 $cm^{-1}$ belonged to the bending and asymmetrical stretching vibration of the silicon-methyl bond [25]. The spectrum displayed as line c has all the characteristic peaks appeared in line a and b, indicating that the $SiO_2$ nanospheres are successfully embed in PS/TPU microfibers. Compared with line c, the intensity of characteristic peak of Si–OH reduced rather than disappeared completely in line d since the symmetric and asymmetric stretching vibrations of the free amine $–NH_2$ occur at around 3,400 $cm^{-1}$ [26,27], which suggested that most of silicon hydroxyls on $SiO_2$ surface were successfully functionalized with the $–NH_2$ groups through hydrolysis amino modification that is shown in Fig. 1 [22].

### 3.2. Cr(VI) adsorption performance by static experiments

The modification reaction conditions, such as temperature and time, APTES concentration, are of great importance in adsorption capacity. In order to obtain high adsorption capacity ($q_e$), modification reaction conditions required to be optimized. The relationships of $q_e$ and reaction temperature and time are given in Fig. 6a. In this study, the optimal hydrolysis amino modification temperature and time are 50°C and

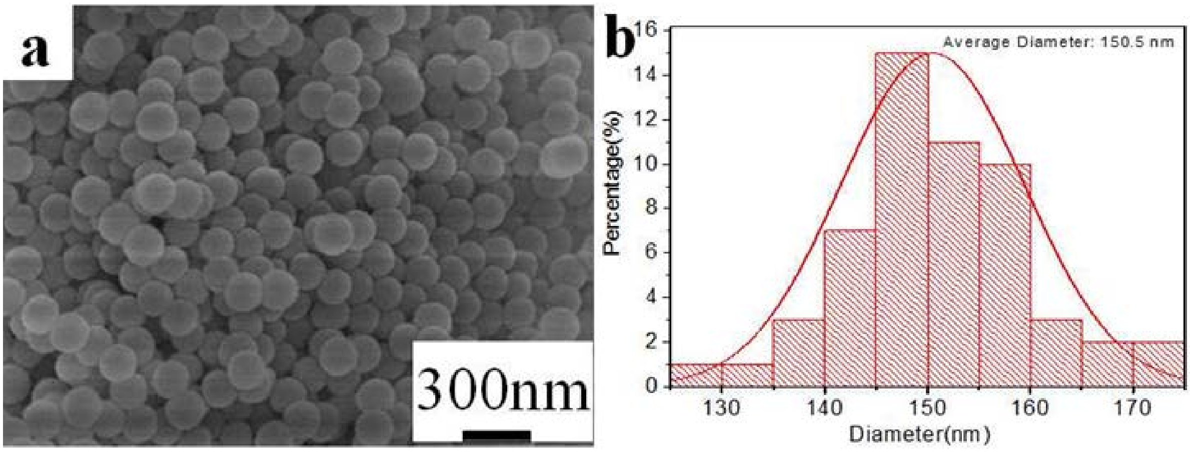

Fig. 2. (a) SEM image and (b) diameter histogram of synthesized $SiO_2$ nanospheres.

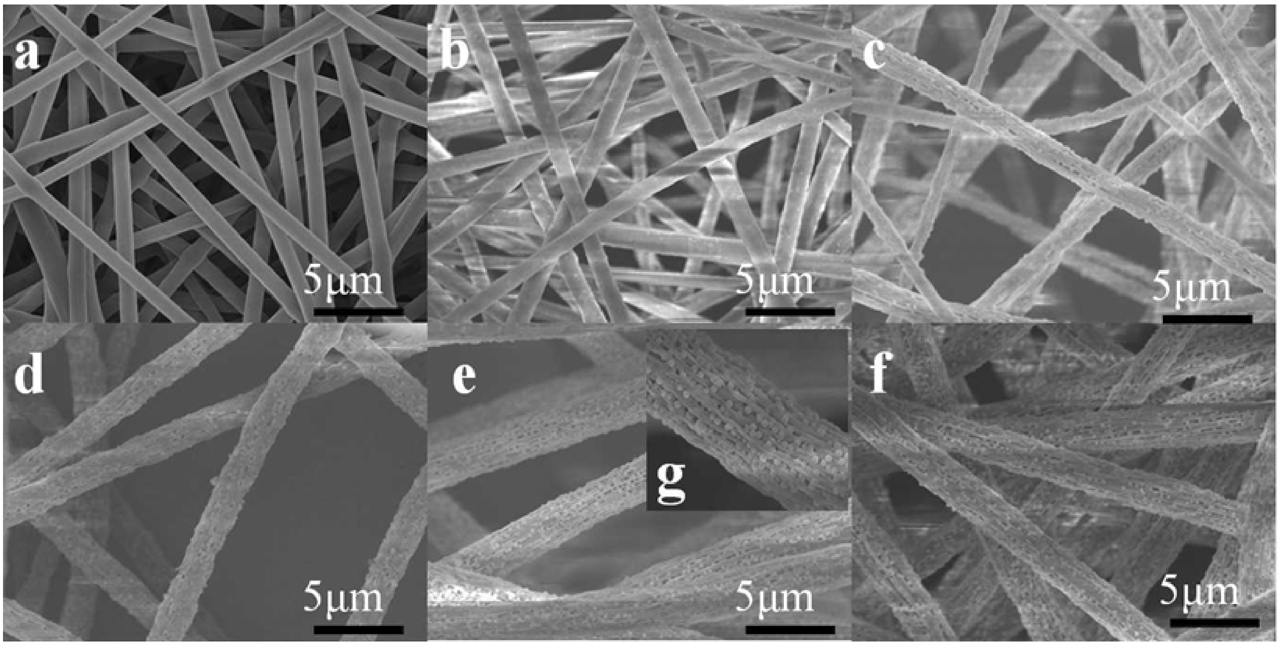

Fig. 3. SEM images of pristine PS/TPU microfiber membrane (a) and PS/TPU@$SiO_2$ microfiber membranes with varying $SiO_2$ NPs contents: (b) 0.5 g, (c) 1.0 g, (d) 1.5 g, (e) 2.0 g and (f) 2.5 g; Inset is the high magnification image.

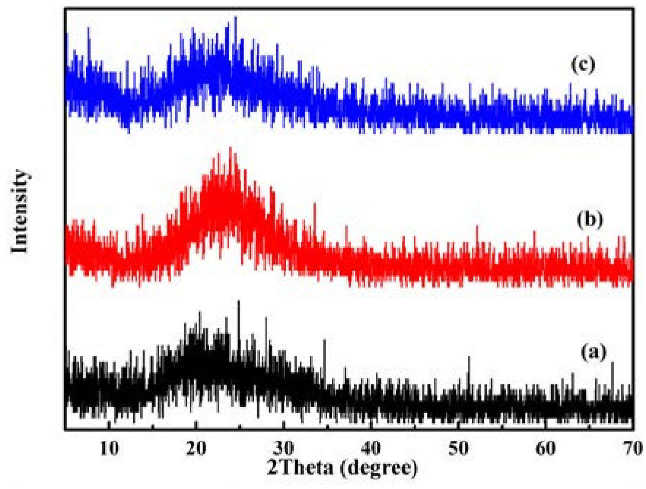

Fig. 4. XRD patterns of (a) PS/TPU microfiber membrane, (b) $SiO_2$ nanosphere and (c) PS/TPU@$SiO_2$ composite microfiber membrane.

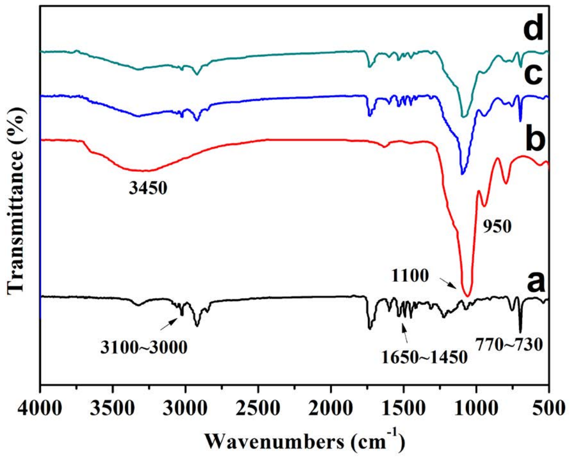

Fig. 5. FT-IR spectra of (a) PS/TPU microfiber membranes, (b) $SiO_2$ NPs, (c) PS/TPU@$SiO_2$ composite microfiber membranes and (d) $NH_2$-grafting PS/TPU@$SiO_2$ composite microfiber membranes.

24 h, respectively. When the hydrolysis reaction occurred under variable temperatures (40°C, 50°C or 60°C), the removal performance of Cr(VI) by the modified PS/TPU@$SiO_2$ composite microfiber membrane first increased with increasing temperature, and reached a maximum value at 50°C, then decreasing slightly with further increases in temperature. This is because the kinetics of the APTES will accelerate by increasing the mobility of APTES in reaction system [28] and an increase in interactions between APTES molecules and the $SiO_2$ surface hydroxyl groups, facilitating APTES binding to the $SiO_2$ surface. However, a higher temperature did not lead to increased Cr(VI) removal. A similar trend was reported for the effect of reaction temperature on reactive dyes adsorption capacity by APTES modified attapulgite [26] and on Hg(II) adsorption capacity by APTES modified active carbon [29].

Further, the adsorption capacity increased first and then decreased with increasing APTES concentration, as presented in Fig. 6b. A same phenomenon has been reported by Xue et al. [26]. Under the hydrolysis condition of 50°C and 24 h, the highest adsorption performance for Cr(VI) was obtained at 2% APTES (volume ratio) content. When the content of APTES increased continuously, the excess APTES in the system might be expected to self-polymerize after hydrolysis to form a Si–O–Si backbone [26]. This will prevent silanol groups

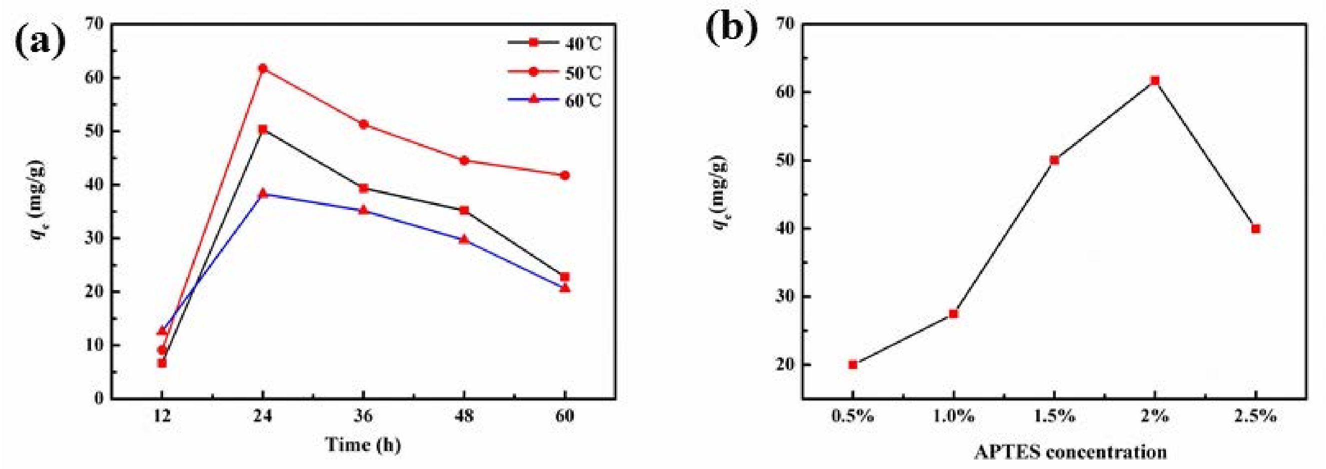

Fig. 6. Effect of modification conditions on the adsorption capacity of Cr(VI): (a) reaction temperature and time and (b) APTES concentration.

from forming hydrogen bonds with the surface hydroxyl groups of $SiO_2$ nanospheres. Thus, the $–NH_2$ on the modified composite membrane surface would reduce with an excess of APTES, and lead to a reduced Cr(VI) adsorption capacity. In the following Cr(VI) removal experiments, $NH_2$-grafting PS/TPU@$SiO_2$ composite microfiber membrane was obtained by hydrolysis with 2% APTES at 50°C and 24 h.

The adsorption of Cr(VI) from aqueous solution by $NH_2$-grafting PS/TPU@$SiO_2$ composite microfiber membrane was investigated by a batch method. The $NH_2$-grafting PS/TPU@$SiO_2$ composite microfiber membrane exhibited a unique affinity for Cr(VI). Fig. 7a shows the time profile of Cr(VI) removal with 0.01 g of composite membrane at room temperature. Refer to the results of ICP-AES, the Cr content sharply decreases from 40 to 20.8 mg $L^{-1}$ in first 24 h, and then the Cr content nearly keeps constant. From the curve in Fig. 7a, the process of Cr(VI) removal can be divided into two stages: the first 24 h and the next 8 h. Apparently, the adsorption could reach equilibrium within 24 h. The first stage of removing Cr(VI) shows higher adsorption efficiency, which is probably due to the high Cr(VI) concentration and a lot of active sites for adsorption. There is an equilibrium in second stage, which may due to the consumption of active sites on the membrane surface. Moreover, the equilibrium Cr(VI) adsorption capacity of composite membrane is found to be 57.73 mg $g^{-1}$ when the initial Cr(VI) concentration is 40.0 mg $L^{-1}$.

According to the equilibrium adsorption time, the experimental data were fitted with both pseudo-first-order and pseudo-second-order kinetic models to investigate the kinetic parameters of Cr(VI) adsorption onto $NH_2$-grafting PS/TPU@$SiO_2$ composite microfiber membrane. The kinetic curves are shown in Figs. 7b and c, respectively. Eqs. (2) and (3) are the pseudo-first-order and pseudo-second-order kinetic models, respectively [4].

$$\ln\left(q_e - q_t\right) = \ln q_e - k_1 t \tag{2}$$

$$\frac{t}{q_t} = \frac{1}{k_2 q_e^2} + \frac{t}{q_e} \tag{3}$$

where $q_e$ is the adsorption capacity (mg $g^{-1}$) of ions on the adsorbent at equilibrium, $q_t$ is the adsorption capacity (mg $g^{-1}$) of ions on the adsorbent at time $t$ (h), $k_1$ is the pseudo-first-order rate constant ($h^{-1}$) and $k_2$ is the pseudo-second-order rate constant (g $mg^{-1}$ $h^{-1}$). $k_1$ can be obtained from the slope of a straight line fitted by the plot of $\ln(q_e - q_t)$ vs. $t$ and $k_2$ can be determined from the intercept of plot of $t/q_t$ against $t$. These kinetic parameters and correlation coefficient $R^2$ were calculated and are shown in Table 1. It is observed that the correlation coefficient $R^2$ for pseudo-second-order kinetic model is above 0.99, indicating that the adsorption of Cr(VI) onto $NH_2$-grafting PS/TPU@$SiO_2$ composite microfiber membrane can be described well by the pseudo-second-order kinetic model.

For the isothermal adsorption study, 0.01 g PTS-2 was taken as sample and set the initial Cr(VI) concentration from 10 to 80 mg $L^{-1}$. Langmuir and Freundlich isotherm models are widely used to describe the adsorption isotherms data, in order to better understand the adsorption properties and interactions. Their linear equations are as follows [18]:

Langmuir isotherm (homogeneous and monolayer adsorption):

$$\frac{C_e}{q_e} = \frac{C_e}{q_{\max}} + \frac{1}{bq_{\max}} \tag{4}$$

Freundlich isotherm (heterogeneous and multilayer adsorption):

$$q_e = K_f C_e^{n_f} \tag{5}$$

where $q_e$ is the equilibrium adsorption capacity (mg $g^{-1}$), $C_e$ is the equilibrium concentration (mg $L^{-1}$), and $q_m$ (mg $g^{-1}$) and $b$ (L $mg^{-1}$) are Langmuir constants related to maximum adsorption capacity and binding energy, respectively; $K_f$ and $n$ are empirical constants that indicate the Freundlich constant and heterogeneity factor, respectively. The linear fitting plots are shown in Figs. 7d and e and the data are listed in Table 1. By comparing the correlation coefficients, the Langmuir model fitted well with the isotherms data

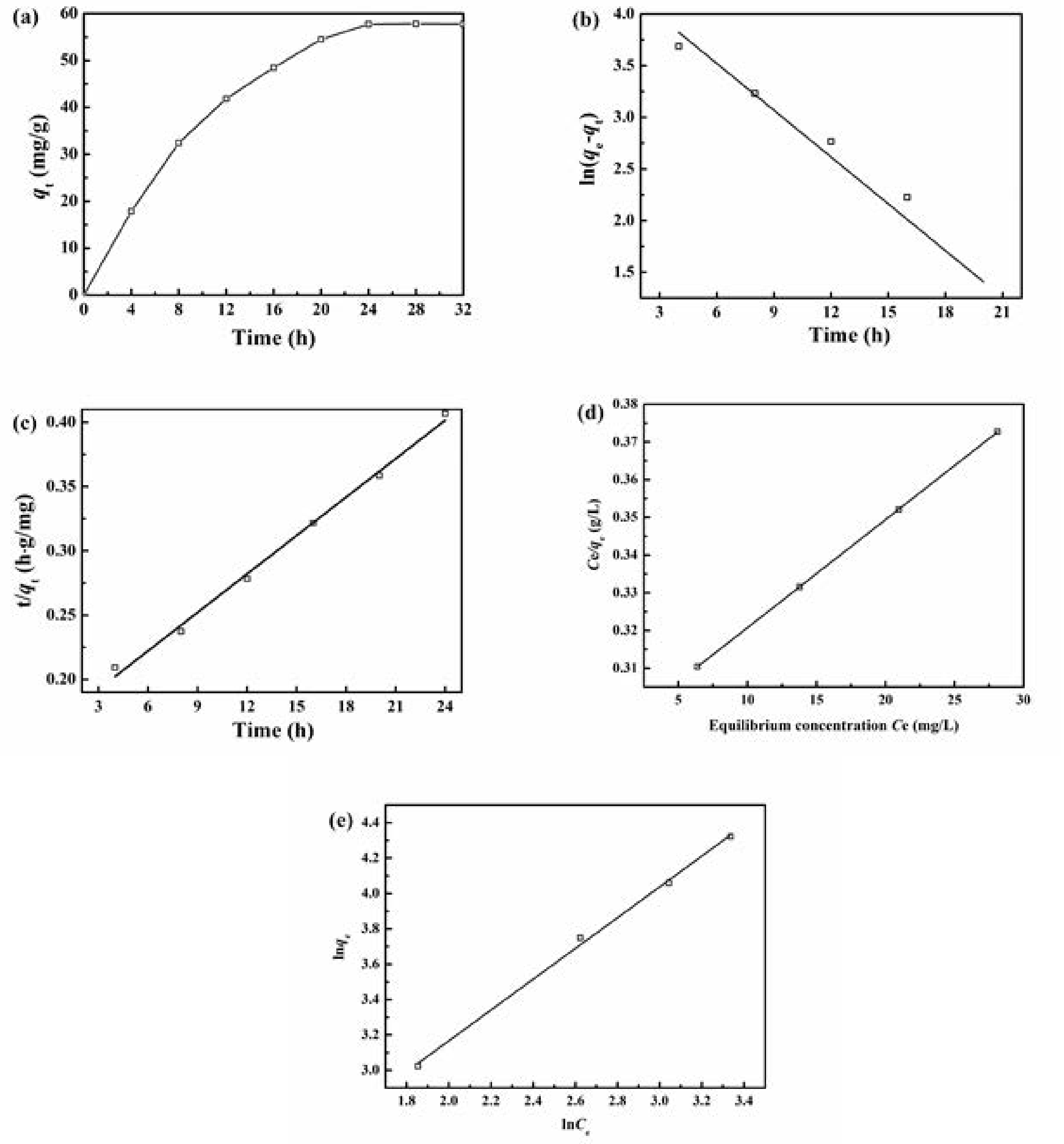

Fig. 7. (a) Adsorption curve of Cr(VI) removal onto amino-grafted PS/TPU@$SiO_2$ composite microfiber membrane, (b) and (c) linear fitting plots of adsorption kinetics ($c_0$ = 40 mg $L^{-1}$) and (d) and (e) linear fitting by Langmuir and Freundlich isotherms at 298 K.

Table 1
Adsorption kinetics and isotherm adsorption data for Cr(VI) removal onto PTS-2

| Adsorbent | Pseudo-first-order model | | | Pseudo-second-order model | | |
|---|---|---|---|---|---|---|
| | $q_e$ (mg $g^{-1}$) | $k_1$ ($h^{-1}$) | $R^2$ | $q_e$ (mg $g^{-1}$) | $k_2$ (g $mg^{-1}$ $h^{-1}$) | $R^2$ |
| PTS-2 | 83.63 | $2.51 \times 10^{-3}$ | 0.9497 | 57.73 | $4.43 \times 10^{-2}$ | 0.9945 |
| | Langmuir isotherm | | | Freundlich isotherm | | |
| | $q_{\max}$ (mg $g^{-1}$) | $b$ (L $mg^{-1}$) | $R^2$ | $K_f$ | $n$ | $R^2$ |
| PTS-2 | 348.43 | $9.82 \times 10^{-3}$ | 0.9991 | 4.15 | 1.15 | 0.9764 |

of Cr(VI) removal onto PTS-2. Comparing with previous literature about functionalized polymer/silica composite electrospun membrane [22], such as $NH_2$-functionalized CA/$SiO_2$ membrane that exhibited the maximal adsorption capacity of Cr(VI) was 19.46 mg $g^{-1}$, our work presents a much better adsorbent with the higher adsorption capacity ($q_m$ = 348.43 mg $g^{-1}$).

### 3.3. Regeneration and recyclability of adsorbent

For practical application, the regeneration and recycling of the adsorbent are important and indispensible. Because of the self-supporting structure and macroscopic size of electrospun microfiber membrane, the collection of Cr(VI)-adsorbed $NH_2$-grafting PS/TPU@$SiO_2$ membrane was very convenient and fast. We took out the Cr(VI) saturated membrane directly from solution and treated it with NaOH solution for 6 h, which can effectively induce the desorption of Cr(VI) [5,22]. The desorption was supposed to be attributed to the elimination of protonation of both $–NH_2$ groups and $Cr_2O_7^{2-}$ [2], because the removal of Cr(VI) was most ascribed to the electrostatic attraction of protonated amine groups ($–NH_3^+$) and Cr(VI) species ($HCrO_4^-$), which will be discussed in the following section. The Cr species remained on the membrane could be washed away by the following rinse with deionized water. We used the same batch of composite membrane to adsorb Cr(VI) (initial concentration of 10 mg $L^{-1}$) for three consecutive cycles (Fig. 8) and the removal efficiency was 86.90% at the first cycle and then slightly decreased to 67.58% at the third cycle. After three times recycling, the Cr removal efficiency still remains above ~60%, indicating a good recyclability.

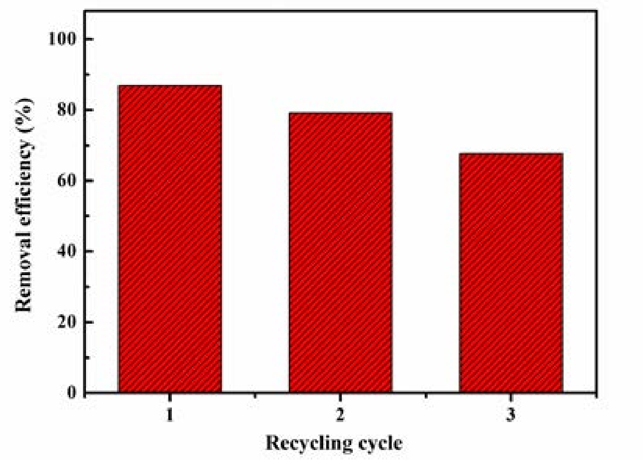

Fig. 8. Regeneration and recyclability study of $NH_2$-grafting PS/TPU@$SiO_2$ composite microfiber membrane with three cycles. The initial concentration of Cr(VI) solution was 10 mg $L^{-1}$. The contact time was 24 h for each cycle. The adsorbent dosage was 0.01 g.

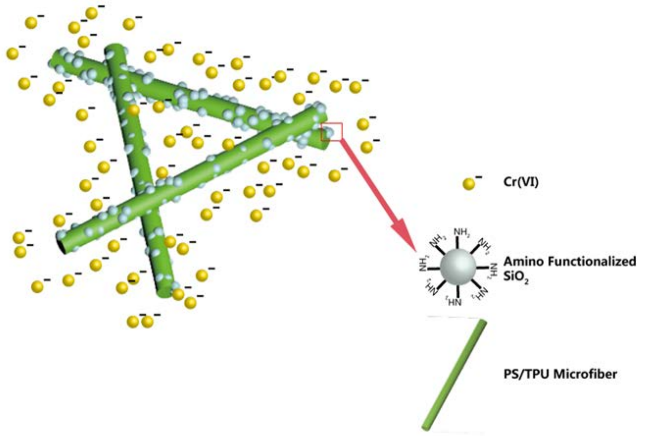

Fig. 9. Mechanism for Cr(VI) removal by $NH_2$-grafting PS/TPU@$SiO_2$ composite microfiber membrane.

### 3.4. Cr(VI) removal mechanism

It is known that the initial pH would govern the surface charge of adsorbent as well as metal ions. There are plenty of amine groups ($–NH_2$) grafted on the surface of composite membrane. When the solution is acidic (pH = 2 in this work), $–NH_2$ on the modified composite membrane can be protonated and exist in the positively charged form ($–NH_3^+$) in aqueous solution [26]. On the other hand, the Cr(VI) would mainly exist in the form of negatively charged $HCrO_4^-$ [4]. Thus, $NH_2$-grafting composite membrane adsorbs Cr(VI) by electrostatic attractive interactions, as shown in Fig. 9. This indicates that surface modification by the APTES significantly enhanced the adsorption capacity of composite electrospun microfiber membrane for Cr(VI) from aqueous solution.

## 4. Conclusions

This study fabricated PS/TPU@$SiO_2$ composite microfiber membrane with micro/nano architecture and modified it with an amine-terminated organosilicon (3-aminopropyltriethoxysilane, APTES) to graft amino groups onto membrane surface, which substantially enhanced the adsorption capacity of Cr(VI) from aqueous solution. The optimal conditions for surface modification of electrospun membrane were achieved by using 2% APTES with ethanol, and the reaction was conducted at 50°C and 24 h. This successive amino-functionalization of PS/TPU@$SiO_2$ composite microfiber membrane exhibited considerable efficiency (>86%) and good recyclability toward Cr(VI) removal from aqueous solution. In the batch adsorption, the adsorption behavior followed the pseudo-second-order kinetic model and Langmuir isotherm adsorption model. Therefore, this work provides a facile and effective approach for the fabrication of multi-dimensional composite electrospun membrane, which can be potentially applied in the environmental remediation, such as Cr(VI) removal from surface water.

## Acknowledgments

This work was supported by the National Natural Science Foundation of China (grant numbers 21274006, 51503005), Beijing Science and Technology Leading Talent Project (grant number Z161111000490000), Beijing Excellent Talent Training

Subsidy Program (grant number 2017000020124G089), Special Funds of Beijing Institute of Fashion Technology (grant number BIFTQG201807), Talent introduction project of Beijing Institute of Fashion Technology (2017A-19), Cross Training of High-Caliber Talents Project of Beijing Municipal Institutions - the "Real Culture" Program and National Undergraduate Innovation and Entrepreneurship Training Program.

## References

[1] C.E. Barrera-Díaz, V. Lugo-Lugo, B. Bilyeu, A review of chemical, electrochemical and biological methods for aqueous Cr(VI) reduction, J. Hazard. Mater., 223 (2012) 1–12.

[2] G.-R. Xu, J.-N. Wang, C.-J. Li, Preparation of hierarchically nanofibrous membrane and its high adaptability in hexavalent chromium removal from water, Chem. Eng. J., 198 (2012) 310–317.

[3] Y. Li, S. Zhu, Q. Liu, Z. Chen, J. Gu, C. Zhu, T. Lu, D. Zhang, J. Ma, N-doped porous carbon with magnetic particles formed in situ for enhanced Cr(VI) removal, Water Res., 47 (2013) 4188–4197.

[4] Y. Zheng, W. Wang, D. Huang, A. Wang, Kapok fiber oriented-polyaniline nanofibers for efficient Cr(VI) removal, Chem. Eng. J., 191 (2012) 154–161.

[5] N. Wu, H. Wei, L. Zhang, Efficient removal of heavy metal ions with biopolymer template synthesized mesoporous titania beads of hundreds of micrometers size, Environ. Sci. Technol., 46 (2012) 419–425.

[6] L. Sun, L. Zhang, C. Liang, Z. Yuan, Y. Zhang, W. Xu, J. Zhang, Y. Chen, Chitosan modified $Fe^0$ nanowires in porous anodic alumina and their application for the removal of hexavalent chromium from water, J. Mater. Chem., 21 (2011) 5877–5880.

[7] L.S. Zhong, J.S. Hu, H.P. Liang, A.M. Cao, W.G. Song, L.J. Wan, Self-assembled 3D flowerlike iron oxide nanostructures and their application in water treatment, Adv. Mater., 18 (2006) 2426–2431.

[8] Y. Lin, W. Cai, X. Tian, X. Liu, G. Wang, C. Liang, Polyacrylonitrile/ferrous chloride composite porous nanofibers and their strong Cr-removal performance, J. Mater. Chem., 21 (2011) 991–997.

[9] Y.-C. Chang, D.-H. Chen, Preparation and adsorption properties of monodisperse chitosan-bound $Fe_3O_4$ magnetic nanoparticles for removal of Cu(II) ions, J. Colloid Interface Sci., 283 (2005) 446–451.

[10] Z. Ai, Y. Cheng, L. Zhang, J. Qiu, Efficient removal of Cr(VI) from aqueous solution with Fe@$Fe_2O_3$ core–shell nanowires, Environ. Sci. Technol., 42 (2008) 6955–6960.

[11] Y. Feng, J.-L. Gong, G.-M. Zeng, Q.-Y. Niu, H.-Y. Zhang, C.-G. Niu, J.-H. Deng, M. Yan, Adsorption of Cd (II) and Zn (II) from aqueous solutions using magnetic hydroxyapatite nanoparticles as adsorbents, Chem. Eng. J., 162 (2010) 487–494.

[12] J. Wang, S. Zheng, Y. Shao, J. Liu, Z. Xu, D. Zhu, Amino-functionalized $Fe_3O_4$@$SiO_2$ core–shell magnetic nanomaterial as a novel adsorbent for aqueous heavy metals removal, J. Colloid Interface Sci., 349 (2010) 293–299.

[13] R. Wu, J. Qu, Y. Chen, Magnetic powder MnO–$Fe_2O_3$ composite—a novel material for the removal of azo-dye from water, Water Res., 39 (2005) 630–638.

[14] S. Wu, F. Li, Y. Wu, R. Xu, G. Li, Preparation of novel poly(vinyl alcohol)/$SiO_2$ composite nanofiber membranes with mesostructure and their application for removal of $Cu^{2+}$ from waste water, Chem. Commun., 46 (2010) 1694–1696.

[15] S. Wu, F. Li, H. Wang, L. Fu, B. Zhang, G. Li, Effects of poly (vinyl alcohol) (PVA) content on preparation of novel thiol-functionalized mesoporous PVA/$SiO_2$ composite nanofiber membranes and their application for adsorption of heavy metal ions from aqueous solution, Polymer, 51 (2010) 6203–6211.

[16] R. Zhao, X. Li, B. Sun, Y. Li, Y. Li, R. Yang, C. Wang, Branched polyethylenimine grafted electrospun polyacrylonitrile fiber membrane: a novel and effective adsorbent for Cr(VI) remediation in wastewater, J. Mater. Chem. A, 5 (2017) 1133–1144.

[17] R. Zhao, X. Li, B. Sun, H. Ji, C. Wang, Diethylenetriamine-assisted synthesis of amino-rich hydrothermal carbon-coated electrospun polyacrylonitrile fiber adsorbents for the removal of Cr(VI) and 2,4-dichlorophenoxyacetic acid, J. Colloid Interface Sci., 487 (2017) 297–309.

[18] R. Zhao, X. Li, Y. Li, Y. Li, B. Sun, N. Zhang, S. Chao, C. Wang, Functionalized magnetic iron oxide/polyacrylonitrile composite electrospun fibers as effective chromium (VI) adsorbents for water purification, J. Colloid Interface Sci., 505 (2017) 1018–1030.

[19] C.-J. Li, Y.-J. Li, J.-N. Wang, J. Cheng, PA6@$Fe_xO_y$ nanofibrous membrane preparation and its strong Cr (VI)-removal performance, Chem. Eng. J., 220 (2013) 294–301.

[20] X. Li, N. Wang, G. Fan, J. Yu, J. Gao, G. Sun, B. Ding, Electreted polyetherimide-silica fibrous membranes for enhanced filtration of fine particles, J. Colloid Interface. Sci., 439 (2015) 12–20.

[21] X. Wang, L. Dou, Z. Li, L. Yang, J. Yu, B. Ding, Flexible hierarchical $ZrO_2$ nanoparticle-embedded $SiO_2$ nanofibrous membrane as a versatile tool for efficient removal of phosphate, ACS Appl. Mater. Interfaces, 8 (2016) 34668–34676.

[22] A.A. Taha, Y.-N. Wu, H. Wang, F. Li, Preparation and application of functionalized cellulose acetate/silica composite nanofibrous membrane via electrospinning for Cr(VI) ion removal from aqueous solution, J. Environ. Manage., 112 (2012) 10–16.

[23] X.-D. Wang, Z.-X. Shen, T. Sang, X.-B. Cheng, M.-F. Li, L.-Y. Chen, Z.-S. Wang, Preparation of spherical silica particles by Stöber process with high concentration of tetra-ethyl-orthosilicate, J. Colloid Interface Sci., 341 (2010) 23–29.

[24] N. Wang, Y. Si, N. Wang, G. Sun, M. El-Newehy, S.S. Al-Deyab, B. Ding, Multilevel structured polyacrylonitrile/silica nano-fibrous membranes for high-performance air filtration, Sep. Purif. Technol., 126 (2014) 44–51.

[25] J. Sheng, Y. Xu, J. Yu, B. Ding, Robust fluorine-Free superhydrophobic amino-silicone oil/$SiO_2$ modification of electrospun polyacrylonitrile membranes for waterproof-breathable application, ACS Appl. Mater. Interfaces, 9 (2017) 15139–15147.

[26] A. Xue, S. Zhou, Y. Zhao, X. Lu, P. Han, Effective $NH_2$-grafting on attapulgite surfaces for adsorption of reactive dyes, J. Hazard. Mater., 194 (2011) 7–14.

[27] N. Srivastava, A.K. Thakur, V.K. Shahi, Phosphorylated cellulose triacetate–silica composite adsorbent for recovery of heavy metal ion, Carbohydr. Polym., 136 (2016) 1315–1322.

[28] J.A. Howarter, J.P. Youngblood, Optimization of Silica Silanization by 3-Aminopropyltriethoxysilane, Langmuir, 22 (2006) 11142–11147.

[29] J. Zhu, J. Yang, B. Deng, Enhanced mercury ion adsorption by amine-modified activated carbon, J. Hazard. Mater., 166 (2009) 866–872.

## Supplementary Information

According to the literature, Cr(VI) removal highly depends on the solution pH, and an acidic environment favors their removal. Similar phenomenon was observed in this study. The adsorption capacity of Cr(VI) decreased from 57.73 to 5.21 mg $g^{-1}$ when the pH values increased from 2 to 10. Therefore, the pH values of Cr(VI) initial solutions were adjusted to 2.0 during all the following Cr(VI) removal experiments.

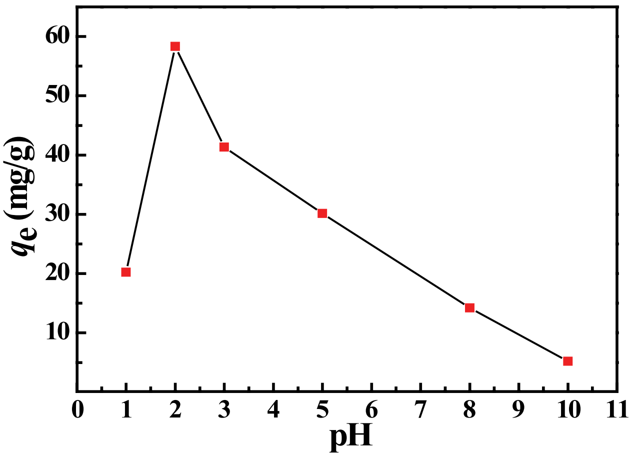

Fig. S1. Influence of solution pH on the Cr(VI) removal.